Experimental Eye Research 119 (2014) 70–76

Contents lists available at ScienceDirect

Experimental Eye Research

journal homepage: www.elsevier.com/locate/yexer

Effects of a Schlemm canal scaffold on collector channel ostia in human anterior segments

Murray A. Johnstone [a,1], Hady Saheb [b,2], Iqbal Ike K. Ahmed [c,3], Thomas W. Samuelson [d,e,4], Andrew T. Schieber [f,5], Carol B. Toris [g,*]

[a] Department of Ophthalmology, University of Washington, Seattle, WA, USA
[b] Department of Ophthalmology, McGill University, Montreal, QC, Canada
[c] Department of Ophthalmology and Visual Sciences, University of Toronto, Mississauga, 3200 Erin Mills Parkway, Unit 1, Mississauga, ON, Canada
[d] Department of Ophthalmology, University of Minnesota, Minneapolis, MN 55404, USA
[e] Minnesota Eye Consultants, 710 East 24th Street, Suite 100, Minneapolis, MN 55404, USA
[f] Ivantis Inc., 38 Discovery, Suite 150, Irvine, CA 92618, USA
[g] Department of Ophthalmology and Visual Sciences, University of Nebraska Medical Center, Omaha, NE 68198-5840, USA

ARTICLE INFO

Article history:
Received 16 August 2013
Accepted in revised form 12 December 2013
Available online 24 December 2013

Keywords:
Schlemm's canal
glaucoma
drainage device
trabecular meshwork
collector channels

ABSTRACT

This study evaluates the morphologic effect of the implantation of two different sizes of the Hydrus microstent on the outer wall of Schlemm's canal (SC) and collector channel (CC) ostia. Twelve human eyes were dissected at the equator removing the iris, lens, ciliary body and vitreous. The cornea was excised with a corneal trephine exposing a direct view of the angle while leaving the trabecular meshwork (TM) intact. The Hydrus delivery system was used to deliver microstents of 8 mm and 15 mm in length into SC. Following delivery, the tissues were immediately immersed in fixative. After tissue fixation, the microstents were gently lifted out of SC through the TM leaving a small slit opening in the TM. The slit opening was widened by gently dissecting the entire TM. Control eyes underwent dissection before fixation by gently removing the TM exposing the outer wall of SC. The tissues were prepared for scanning electron microscopy (SEM). The external wall of SC was imaged using SEM and were reviewed with particular attention focused on the distribution of irregular particulate matter (IPM), the shape of the CC ostia and the health of the SC endothelium. Three eyes received the 8 mm microstent, two the 15 mm microstent and 6 eyes served as controls. Five of the controls had reported histories of glaucoma while all other eyes were normal. All eyes showed evidence of removal of the trabecular meshwork revealing the external wall of SC. CCs were regularly visible in all eyes and were not obstructed, compressed or their margins disrupted. Nuclear profiles were oriented circumferentially in SC except at regions of CC ostia where they assumed a radial configuration oriented toward the lumen of the CC. The area of microstent contact with SC external wall was examined with SEM and a comparison made between the 8 and 15 mm microstent showing a smaller area of indentation with the 8 mm microstent. The indentations were generally free of particulate debris, were smooth and were devoid of nuclear profiles. In bridged areas adjacent to areas of microstent contact, CCs were identified, appearing patent and intact like those of the control eyes. The eyes receiving 8 mm and 15 mm Hydrus microstents both maintained CC ostia patency but a smaller area of external wall contact was evident from insertion of the 8 mm microstent.

* Corresponding author. Department of Ophthalmology, 985840 Nebraska Medical Center, Omaha, NE 68198-5840, USA. Tel.: +1 402 559 7492; fax: +1 402 559 5368.
E-mail addresses: johnstone.murray@gmail.com (M.A. Johnstone), hady.saheb@mcgill.ca (H. Saheb), ike.ahmed@utoronto.ca (I.I.K. Ahmed), twsamuelson@mneye.com (T. W. Samuelson), aschieber@ivantisinc.com (A.T. Schieber), ctoris@unmc.edu (C.B. Toris).
[1] Tel.: +1 206 719 8520.
[2] Tel.: +1 514 934 1934x35763.
[3] Tel.: +1 905 820 6789.
[4] Tel.: +1 612 813 3607.
[5] Tel.: +1 949 333 1319.

0014-4835
http://dx.doi.org/10.1016/j.exer.2013.12.011

1. Introduction

Intraocular pressure (IOP) lowering is the primary approach used in glaucoma management. Surgically, trabeculectomy and glaucoma drainage devices remain the most common procedures for lowering IOP in open angle glaucoma (Ramulu et al., 2007) by diverting aqueous humor directly into the subconjunctival space (Gedde et al., 2012a). Early wound healing variability as well as late tissue remodeling in this region contribute to complications and failures (Gedde et al., 2012b; Lama and Fechtner, 2003). More recently, procedures without subconjunctival drainage or bleb formation have been developed to circumvent problems associated with diverting aqueous humor to non-physiologic pathways.

Recently, new surgical procedures have been developed to directly enhance the conventional outflow pathway of aqueous humor into Schlemm's canal (SC), to collector channels (CCs) and then through the aqueous veins into the episcleral veins. Canaloplasty (iScience Interventional, Menlo Park, CA) utilizing an ab-externo approach to place a tension suture in SC, Trabectome® (NeoMedix, Inc., Tusin, CA), an ab-interno trabeculotomy, and the iStent® (Glaukos, Inc., Irvine, CA), a self-trephinating ab-interno trabecular microstent are examples of such approaches (Lewis et al., 2007; Francis et al., 2011). Scanning electron microscopy (SEM) has been used recently to evaluate the effect of a microstent placement in a short segment of SC but there is little published data on SC instrumentation by devices that attempt to provide access to a larger region of the canal and associated regional collector channels (Bahler et al., 2012).

Previous studies involving light and SEM have shown that a suture, a round probe (Johnstone and Grant, 1973a) or a round cannula (Smit and Johnstone, 2002) placed in SC causes damage to SC outer wall endothelium, compression of the scleral collagen of the outer wall and morphologic changes at the collector channel ostia. In addition, a sham procedure involving simple probe insertion into, and then removal from, SC was found to cause an immediate marked reduction in aqueous humor outflow, an effect thought to result from physical SC and CC tissue compression and deformation (Johnstone and Grant, 1973a). The microstents described in the present study have a unique geometry designed to avoid extensive compression and deformation of SC external wall tissue. The current SEM study was undertaken to assess the effectiveness in achieving aqueous humor access to CCs while avoiding damage that would negatively impact long-term aqueous humor outflow.

The Hydrus™ microstent (Ivantis, Inc., Irvine, CA) is a novel Schlemm's canal scaffold made of Nitinol (nickel–titanium alloy) delivered through the TM into SC with an ab-interno gonioscopically-guided approach. The implant is a non-luminal open scaffold designed to take advantage of three potentially important mechanisms: 1) TM bypass, 2) a scaffolding effect over multiple clock-hours of SC and 3) dilation and direct access of aqueous humor to CC ostia (Fig. 1). The proximal 1 mm inlet of the microstent provides the TM bypass, permitting direct communication with SC while the portion within SC provides persistent canal dilation and access to CC ostia.

The objective of this study was to evaluate immediate morphological changes within SC and CC after implantation of the Hydrus microstent in human anterior segments. To decide how to best optimize the scaffold design, two sizes of the microstent were evaluated during the development process. Perfusion studies showed similar outflow facility increase in anterior segments between the 8 mm and 15 mm designs (Camras et al., 2012; Gulati et al., 2013). However, the initial 15 mm microstent design was nearly circular resulting in contact with significantly more of the outer wall of SC. Therefore, the current low profile 8 mm microstent was designed with the intent to contact less of the SC outer wall, potentially preserving more CCs (Fig. 1). In the current study, scanning electron microscopy (SEM) was used to examine the mechanical effects of instrumentation of SC outer wall following insertion of the 8 and 15 mm microstents. Controls were compared with the results of inserting the microstent into SC providing a novel view of the acute effects of inserting such devices.

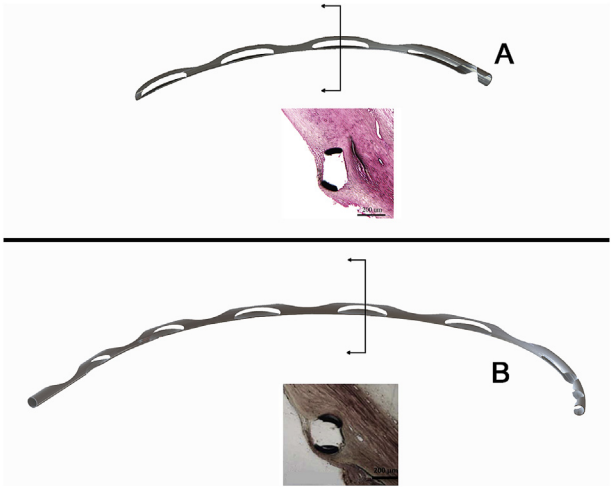

Fig. 1. (A) The 8 mm Hydrus microstent consists of a scaffold of three windows and three spines and an inlet region. The inset is a histological section showing the cross section of a window region. (B) The 15 mm Hydrus microstent consists of a scaffold of five windows and six spines and an inlet region. The inset is a histological section showing the cross section of a window region.

2. Methods

2.1. Tissue preparation

Twelve human eyes were obtained from the San Diego Eye Bank (San Diego, CA) or Lions Eye Institute (Tampa, FL). The mean donor age was 68.3 ± 15.9 years with no reported history of previous ocular surgeries except cataract surgery. Five of the eyes had a reported history of glaucoma. The eyes were wrapped in saline-wetted gauze, placed in moist chambers and shipped on ice. The experiments were completed within a mean of 58.6 ± 18.2 h of death (Table 1). The eyes were bisected at the equator and the iris, lens, ciliary body and vitreous were removed from the anterior segment. The cornea was excised with a corneal trephine exposing a direct view of the angle while leaving the TM intact.

Table 1
Donor information.

Donor sample#	Age	Eye	Post mortem (Hrs)	Glaucoma	Experiment
101	82	OS	46.0	Yes	Control
104	82	OD	46.0	Yes	Control
105	79	OD	33.0	No	Control
108	84	OD	42.0	Yes	Control
109	81	OD	43.5	Yes	Control
111	66	OD	41.0	Yes	Control
113	70	OD	60.0	No	Hydrus 8 mm
114	39	OD	68.0	No	Hydrus 8 mm
115	39	OS	68.0	No	Hydrus 8 mm
116	56	OD	106.0	No	Hydrus 15 mm
117	72	OD	60.0	No	Hydrus 15 mm

2.2. Microstent delivery

The anterior segments were fixtured at an angle comparable to gonioscopic surgery for delivery of the microstents. The Hydrus delivery system was then used to deliver the 8 mm and 15 mm microstents into SC. The delivery cannula penetrated the TM followed by smooth visually controlled advancement of the microstent along the circumference of SC; when approximately 1 mm of the proximal end protruded from the TM into the AC the microstent was released from the delivery system. Proper placement of all microstents in SC was verified because the semitransparent TM tissue permitted direct visualization of the stent as it passed circumferentially along the canal. An experienced Ivantis research scientist performed all the microstent insertions at the Ivantis Inc. (Irvine, CA) facility. Control eyes underwent no manipulation or microstent insertion.

2.3. Fixation and SEM preparation

Following placement of the microstents, the tissues were immediately immersed in fixative consisting of 2.5% glutaraldehyde and 2% paraformaldehyde in phosphate buffer, pH 7.3. The eyes were then shipped to the University of Nebraska Medical Center. All anterior segments were photographed. The 1 mm region of the microstent that protruded from SC was then grasped with forceps and with gentle pressure lifted out of the canal through the TM into the anterior chamber leaving a small slit opening in the TM along the outer wall of SC. The slit opening was widened by gently dissecting the entire TM from both sides of the slit for the entire length of the microstent tract. Control eyes underwent dissection before fixation by gently removing the TM exposing the outer wall of SC. The tissues were washed in Sorenson's buffer, dehydrated in graded ethanols, critical point dried and sputter-coated with 40 nm of gold palladium.

2.4. Scanning electron microscopy

The external wall of SC was imaged using the Quanta 200 scanning electron microscope (from FEI, Hillsboro Oregon; accelerated voltage, 25 KV). A first pass using a magnification of 100× was done to create a panoramic image. The panoramic images were then examined for features such as CC ostia, outer wall impressions or irregular appearance. These unique features once identified in the panoramic images were then imaged using 400× magnification. The SEM images were reviewed with particular attention focused on the distribution of irregular particulate matter (IPM), the shape of the CC ostia and the health of the SC endothelium. The IPM was interpreted as cellular debris associated with tissue disruption related to the microstent passage, its removal, and the removal of the TM to complete unroofing of SC. Typical distribution of IPM was defined as a relatively uniform pattern of IPM observed in areas outside of the microstent tract. Some images demonstrated loss of this normal distribution, and others showed accumulation of IPM at the distal end of the microstent tract where a discrete edge could be identified ("snowplow effect").

All images were reviewed, using the same evaluation to compare control and microstent eyes. Detection of microstent-dependent changes resulted in particular attention to the following issues. The CC ostia were assessed for their shape, presence of artifactual tears, obstruction by IPM or occlusion by compression. The SC endothelial layer was assessed for the presence and orientation of nuclear bulges. The uniform distribution and orientation of nuclear bulges was interpreted as a non-disrupted and presumably intact layer of SC outer wall endothelium. Impressions in the outer wall of SC that appeared to be consistent with the insertion of the microstents were also identified. The width of these impressions were measured and compared to the width of the microstent's expected arc of contact with the outer wall of SC. Representative images were then chosen to illustrate control findings and changes observed with the various microstent insertions.

3. Results

Three eyes received the 8 mm microstent, two the 15 mm microstent and 6 eyes served as controls. Five of the controls had reported histories of glaucoma while all other eyes were normal. Delivery of microstents required only one attempt and was achieved without difficulty in all eyes.

3.1. Controls

The control eyes showed evidence of removal of the trabecular meshwork revealing the external wall of Schlemm's canal (SC) (Fig. 2). Along the external wall of SC collector channel (CC) entrances or ostia were visible. The CC ostia were regularly open with absence of compression of tissue elements. The margins of the entrances had uniform rounded contours indicative of a lack of instrumentation or compression (Minckler and Hill, 2008). Elongated moderately elevated regularly shaped profiles oriented circumferentially in SC were present representative of the nuclei of endothelial cells that are indicative of an intact SC endothelial lining (Allingham et al., 1992).

3.2. Hydrus 8 mm microstent

The eyes receiving the 8 mm Hydrus microstent similarly showed evidence of TM removal revealing SC external wall (Fig. 3). Particulate debris was present but did not occlude SC. Collector channels were regularly visible and were not obstructed, compressed or their margins disrupted. Nuclear profiles were oriented circumferentially in SC except at regions of CC ostia where they assumed a radial configuration oriented toward the lumen of the CC. In one area two collector channels were very close to one another and appeared to have a common lumen. An elevated septum bridged the area between the two visible CC entrances and four attachments that had been separated from the trabecular meshwork converged directly over the bridging septum.

3.3. Hydrus 15 mm microstent

The eyes receiving the 15 mm Hydrus microstent (Fig. 4) had particulate debris present along the external wall but the debris did not occlude the lumen of SC ostia. Ostia of CC again had rounded uniform marginal contours without evidence of compression. Nuclear profiles like those in control eyes were present and maintained a configuration radial to the entrance of CC ostia, consistent with a flow pattern involving aqueous entry to the ostia, findings again consistent with an intact SC endothelial layer in the area (Humphrey, 2008) and typical shear-stress induced cellular alignment in relation to flow (Allingham et al., 1992). In one area, the profile of the edge of a Hydrus microstent could be identified as a result of a uniform depression in the tissue and an absence of normal endothelial cell profiles. Although the indentation associated with the microstent profile compressed tissue immediately adjacent to the CC ostia, the ostia remained open.

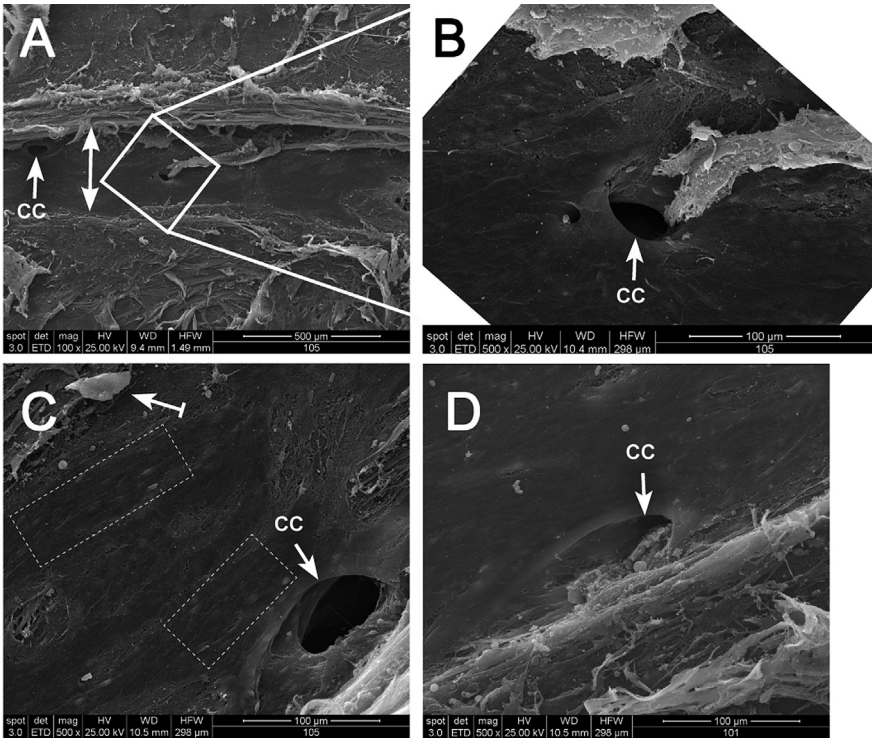

Fig. 2. Scanning electron microscopic image of a control limbal segment with Schlemm's canal (SC) untouched by a microstent. Trabecular meshwork (TM) tissue was removed leaving only a rim of tissue at the margins of the SC external wall. Single arrow points to collector channels (CC). (A) Double arrow spans across the external wall of SC where the upper head of the double arrow contacts the residual rim of trabecular meshwork. (B) Magnification of region outlined in (A). (C) Dotted rectangles outline areas of elongated somewhat spindle-shaped elevations oriented circumferentially in SC consistent with the presence of nuclear profiles typical of an intact endothelium of SC external wall. (D) Collector channel entrance has one sharply demarcated edge and one sloping edge consistent with an oblique entry to SC. Similar CC characteristics are seen in (B) and (C).

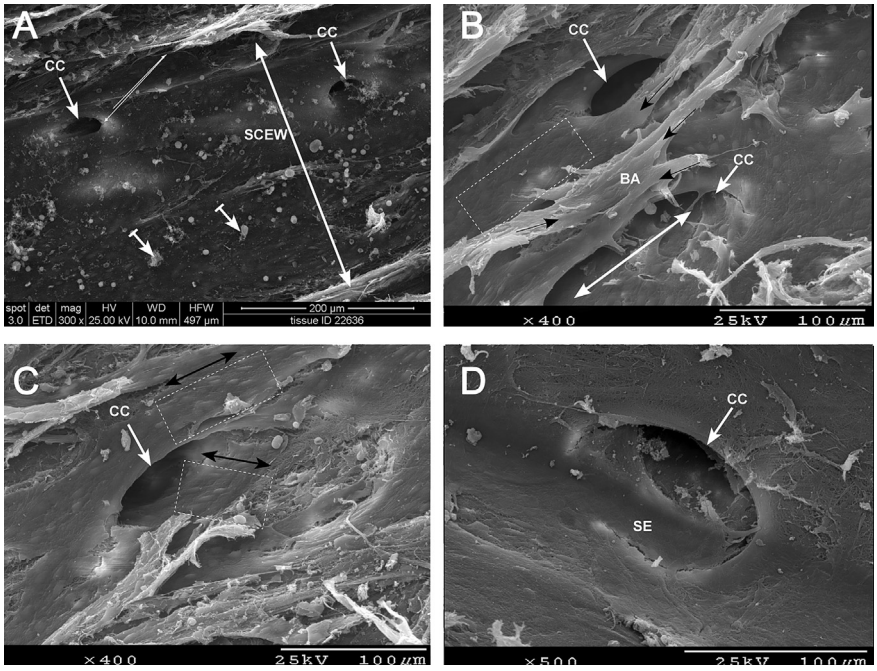

Fig. 3. Scanning electron microscopic image of the outer wall of Schlemm's canal (SC) following insertion and removal of an 8 mm Hydrus microstent Collector channel (cc) ostia are present in panels A–D. Particulate debris is visible particularly in image A (barred arrows). Ostia of collector channels each have a sharp margin on one edge and a sloping one on the opposite edge, consistent with oblique entry to Schlemm's canal. Image B has an upper CC ostia and a lower much longer one with the lumen indicated by the double arrow. The two CC ostia appear to communicate beneath a raised bridging area (BA). Four structures cut away from their attachment to the overlying trabecular meshwork, each converge on the BA (black arrows). In image C, dashed rectangles and associated double arrows denote orientation of nuclear profiles, circumferentially arranged along SC surface in the upper box but radially oriented at a CC ostia in the lower box. The intact but very sloping edge (SE) of the CC ostium (visible in D) resulting from microstent-dependent indentation appearing to compress the lower portion of the ostia while leaving the upper portion open.

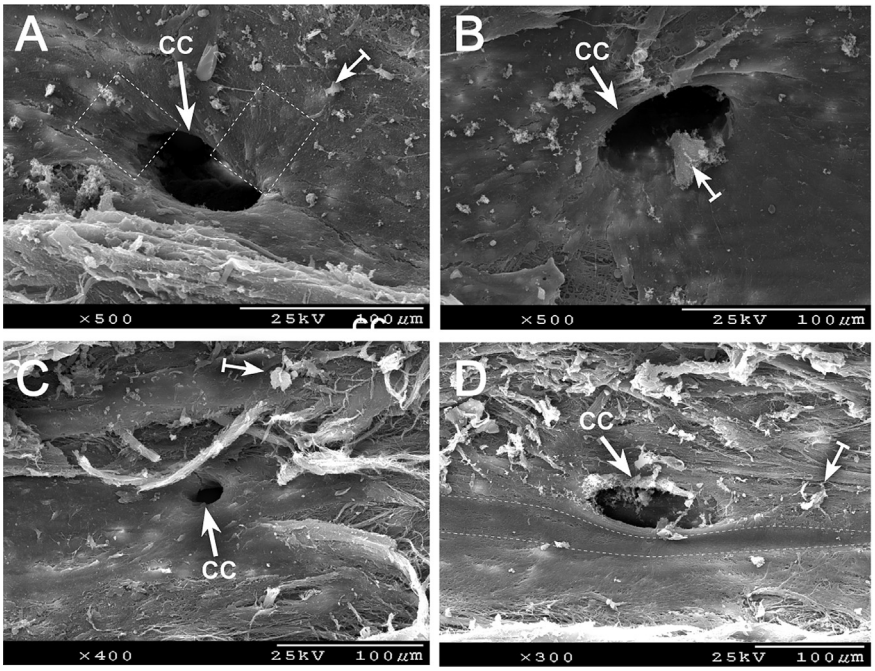

Fig. 4. SEM following insertion of a 15 mm Hydrus microstent. Collector channel ostia (CC) are visible in each of images A–D with the typical oblique entry to SC seen in the controls. Dotted rectangles in image (A) are placed in the same orientation as the radially arranged nuclear bulges of the intact endothelium at the entrance. Particulate debris (barred arrows in A&B) is present but does not occlude the CC ostia. Dotted outline in (D) encompasses microstent indentation adjacent to a CC but ostia of CC remains intact despite close proximity.

3.4. Comparison of area of contact

The area of microstent contact with SC external wall was examined with SEM and a comparison made between the 8 and 15 mm microstent (Fig. 5). Removal of the TM again revealed SC external wall. The microstent profiles could be identified by the presence of geometrically precise curvilinear somewhat crescent-shaped indentations. The indentations were generally free of particulate debris. The surfaces in the indentations were very smooth and were devoid of nuclear profiles. The microstent-caused indentations were especially apparent in the 15 mm microstent where one indentation profile was outlined and an unchanged copy of the outlined area rotated to the adjacent indentation where it fit the indentation perfectly. No CC ostia were apparent in the indentations. The indentation area caused by the 8 mm microstent was much smaller than that caused by the 15 mm microstent and accordingly less of SC external wall had evidence of instrumentation. In un-instrumented bridging areas adjacent to areas of microstent contact, CCs were identified, appearing patent and intact

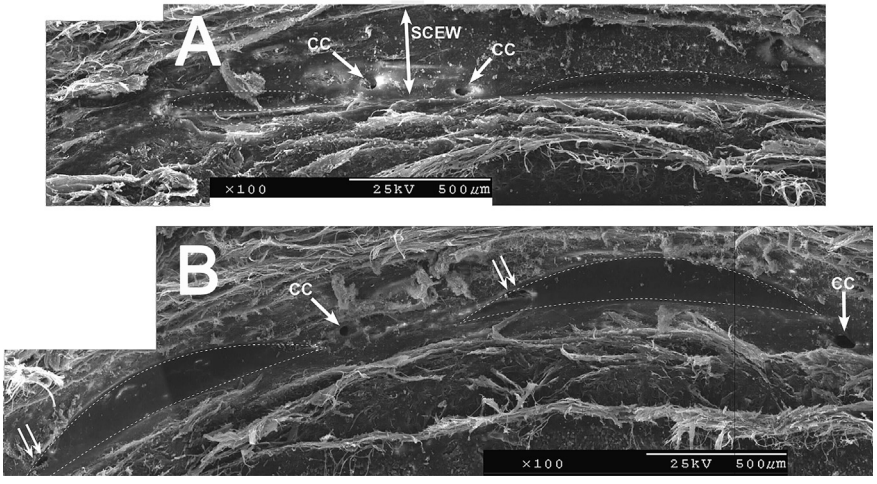

Fig. 5. SEM comparing effects of 8 mm (A) and 15 mm (B) microstent placement in the Schlemm's canal. The Schlemm's canal external wall (SCEW) is visible after trabecular meshwork removal leaving only a rim of trabecular tissue (double arrow in (A). Dotted areas outline microstent generated indentations. Note uniform smooth appearance of outlined indentations without evidence of nuclear profiles. Area of indentation resulting from microstent placement is much smaller with the 8 mm (A) than the 15 mm (B) Hydrus. Collector channel ostia remain patent and have an appearance similar to controls between regions of microstent apposition. Double white arrows point to CC ostia that are located in indentations and appear to be compressed and partially occluded. In image (B) the two indentation areas have an identical superimposable shape consistent with uniform microstent-dependent compression of SCEW.

like those of the control eyes. These bridged areas are shown with pictorial overlay of the Hydrus microstents in Fig. 6.

4. Discussion

The Hydrus microstent is a novel TM bypass and SC scaffold designed to enhance aqueous outflow through the conventional outflow pathway. A larger 15 mm long microstent, which is nearly circular resulting in a higher profile, and a smaller 8 mm long microstent with a low profile design have been developed. Based on this study, both of these devices maintained CC ostia patency. The lower profile 8 mm device with its smaller area of contact resulted in less SC external wall indentation and compression compared to the 15 mm device. The higher profile 15 mm design, which is in more contact with the outer wall of SC, has a greater potential to obstruct CC ostia.

Previous studies of the 8 mm and 15 mm microstent in fresh human anterior segments showed similar increases in outflow facility (Camras et al., 2012; Gulati et al., 2013). Basic fluid dynamic modeling has indicated that dilation of SC with a TM bypass would result in a larger increase in outflow facility than TM bypass alone. Zhou and Smedley (2006) described an increase in circumferential flow within SC with a TM bypass and SC dilation to between 20 μm and 100 μm. An increase in circumferential flow was shown up to 180 degrees from a unidirectional bypass. However, most of the difference occurred in the first 90 degrees with little difference in circumferential flow between 90 and 180 degrees. The lack of substantial circumferential flow indicates that obstruction of only a small number of CC would be enough to negate theoretical expected improvements in outflow. The results of this study show a higher probability for CC obstruction with the larger, longer, more circular profile of the 15 mm microstent when compared to the 8 mm microstent. This could partially explain why experimental perfusions failed to detect any differences in outflow facility increases between the two devices.

Inserting specially designed microstents into SC is a relatively new effort. Previous studies conducted using histologic and SEM analysis involved use of simple round probes (Johnstone and Grant, 1973a) or cannulas (Smit and Johnstone, 2002), making comparisons among studies difficult. Previously published studies involving SC assessment examined the canal by light microscopy and histologic sections rather than the current SEM approach (Dvorak-Theobald, 1934). Another prior study primarily examined different aspects of the microstent interaction with the tissues, mainly biocompatibility (Grierson et al., in press).

The results from this study indicated minimal disruption to normal SC and CC anatomy during the insertion process. Minimizing surgical trauma and disruptions to normal anatomy is likely important to the tolerability of the device. Furthermore, this is likely to reduce the propensity for secondary wound healing issues. The partial circular and open scaffold design of the microstent, along with the manufacturing and polishing design of the microstent resulted in an atraumatic insertion and placement of the implant.

The current study has several limitations of note. Only the immediate impact of mechanical disruption caused to the tissues during insertion of the microstents was evaluated. Biological responses that might occur in the course of wound repair could not be easily predicted from this study. However, a separate study assessed the biocompatibility of the Hydrus microstent in non-human primates and rabbits. This study showed minimal inflammation with no evidence of acute or chronic inflammatory response or fibrosis in the outflow system or in adjacent tissues (Grierson et al., in press).

The post mortem time of the tissue used in this study could have had an impact on the composition of the tissues being evaluated and may have resulted in microstent-dependent tissue changes that would differ from those encountered during in vivo surgery. However, only mechanical interactions with the microstents rather than cellular responses were being evaluated. The mechanical properties of the outer scleral wall and CC ostia do not change significantly within this post-mortem time range (Girard et al., 2007; Schultz et al., 2008). Un-instrumented controls in this study included eyes with glaucoma and one might ask if such eyes differ from normal and would be inappropriate controls. In eyes with elevated pressure, the TM progressively distends into SC until at high IOP it becomes appositional to SC external wall (Johnstone and Grant, 1973b); in fact at high pressures the trabecular tissues can herniate into CC entrances (Battista et al., 2008). Apposition of the TM to Schlemm's canal walls with associated occlusion of CC entrances may be one factor in the glaucoma process. However, this study was limited to assessing the effect of device insertion on Schlemm's canal external wall region, an assessment requiring removal of the TM. Therefore possible glaucoma issues resulting from the relationship between the TM and Schlemm's canal external wall were not a subject of our study.

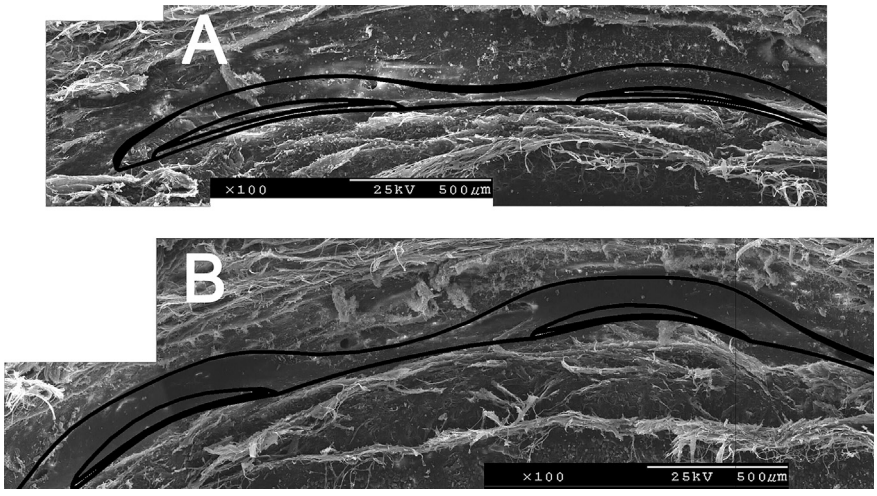

Fig. 6. Pictorial overlay (black solid lines) of 8 mm (A) and 15 mm (B) microstents on the Fig. 5. Scanning electron microscopy image comparing the effects microstent placement on the outer wall of Schlemm's canal (SC). The overlay shows how the microstent bridged an area of the external wall of SC.

Another limitation of the study is the small number of eyes examined with each microstent. A larger number of eyes might have permitted assessing microstent-dependent tissue changes in relation to variations in post mortem time. However, physical indentation of SC external wall and potential obstruction of CC ostia as demonstrated by the 8 mm and 15 mm microstent impressions can be determined with a small number of eyes. Despite the above limitations we feel the current analysis makes it reasonable to conclude that the 8 mm microstent caused less deformation of SC external wall and a correspondingly reduced potential to obstruct CC ostia than the 15 mm microstent.

5. Conclusion

The eyes receiving 8 mm and 15 mm Hydrus microstents both maintained CC ostia patency. A smaller area of contact with resultant reduction of SC external wall indentation-dependent compression resulted from insertion of the 8 mm microstent.

Disclosure

Supported by Ivantis Inc., and an unrestricted grant from Research to Prevent Blindness.

References

Allingham, R.R., de Kater, A.W., Ethier, C.R., Anderson, P.J., Hertzmark, E., Epstein, D.L., 1992. The relationship between pore density and outflow facility in human eyes. Investig. Ophthalmol. Vis. Sci. 33, 1661–1669.

Bahler, C.K., Hann, C.R., Fjield, T., Haffner, D., Heitzmann, H., Fautsch, M.P., 2012. Second-generation trabecular meshwork bypass stent (iStent inject) increases outflow facility in cultured human anterior segments. Am. J. Ophthalmol. 153, 1206–1213.

Battista, S.A., Lu, Z., Hofmann, S., Freddo, T., Overby, D.R., Gong, H., 2008. Reduction of the available area for aqueous humor outflow and increase in meshwork herniations into collector channels following acute IOP elevation in bovine eyes. Investig. Ophthalmol. Vis. Sci. 49, 5346–5352.

Camras, L.J., Yuan, F., Fan, S., Samuelson, T.W., Ahmed, I.K., Schieber, A.T., Toris, C.B., 2012. A novel Schlemm's canal scaffold increases outflow facility in a human anterior segment perfusion model. Investig. Ophthalmol. Vis. Sci. 53, 6115–6121.

Dvorak-Theobald, G., 1934. Schlemm's canal: its anastomoses and anatomic relationships. Trans. Ophthalmol. Soc. 32, 574–595.

Francis, B.A., Singh, K., Lin, S.C., Hodapp, E., Jampel, H.D., Samples, J.R., Smith, S.D., 2011. Novel glaucoma procedures. Ophthalmology 118, 1466–1480.

Gedde, S.J., Schiffman, J.C., Feuer, W.J., Herndon, L.W., Brandt, J.D., Budenz, D.L., 2012a. Treatment outcomes in the Tube Versus Trabeculectomy (TVT) study after five years of follow-up. Am. J. Ophthalmol. 153, 789–803.

Gedde, S.J., Herndon, L.W., Brandt, J.D., Budenz, D.L., Feuer, W.J., Schiffman, J.C., 2012b. Postoperative complications in the Tube Versus Trabeculectomy (TVT) study during five years of follow-up. Am. J. Ophthalmol. 153, 804–814.

Girard, M., Suh, J.K., Hart, R.T., Burgoyne, C.F., Downs, J.C., 2007. Effects of storage time on the mechanical properties of rabbit peripapillary sclera after enucleation. Curr. Eye. Res. 32, 465–470.

Grierson, I., Saheb, H., Kahook, M.Y., Johnstone, M.A., Ahmed, I.I., Schieber, A.T., Toris, C.B., 2013 Nov 14. A novel Schlemm's canal scaffold: histologic observations. J Glaucoma (in press) (Epub ahead of print).

Gulati, V., Fan, S., Hays, C.L., Samuelson, T.W., Ahmed, I.K., Toris, C.B., 2013. A novel 8 mm Schlemm's canal scaffold reduces outflow resistance in a human anterior segment perfusion model. Investig. Ophthalmol. Vis. Sci. 54, 1698–1704.

Humphrey, J.D., 2008. Vascular adaptation and mechanical homeostasis at tissue, cellular, and sub-cellular levels. Cell Biochem. Biophys. 50, 53–78.

Johnstone, M.A., Grant, W.M., 1973a. Microsurgery of Schlemm's canal and the human aqueous outflow system. Am. J. Ophthalmol. 76, 906–917.

Johnstone, M.A., Grant, W.G., 1973b. Pressure-dependent changes in structures of the aqueous outflow system of human and monkey eyes. Am. J. Ophthalmol. 75, 365–383.

Lama, P.J., Fechtner, R.D., 2003. Antifibrotics and wound healing in glaucoma surgery. Surv. Ophthalmol. 48, 314–346.

Lewis, R.A., von Wolff, K., Tetz, M., Korber, N., Kearney, J.R., Shingleton, B., Samuelson, T.W., 2007. Canaloplasty: circumferential viscodilation and tensioning of Schlemm's canal using a flexible microcatheter for the treatment of open-angle glaucoma in adults: interim clinical study analysis. J. Cataract Refract. Surg. 33, 1217–1226.

Minckler, D.S., Hill, R.A., 2008. Use of novel devices for control of intraocular pressure. Exp. Eye Res. 88, 792–798.

Ramulu, P.Y., Corcoran, K.J., Corcoran, S.L., Robin, A.L., 2007. Utilization of various glaucoma surgeries and procedures in Medicare beneficiaries from 1995 to 2004. Ophthalmology 114, 2265–2270.

Schultz, D.S., Lotz, J.C., Lee, S.M., Trinidad, M.L., Stewart, J.M., 2008. Structural factors that mediate scleral stiffness. Investig. Ophthalmol. Vis. Sci. 49, 4232–4236.

Smit, B., Johnstone, M.A., 2002. Effects of viscoelastic injection into Schlemm's canal in primate and human eyes. Potential relevance to viscocanalostomy. Ophthalmology 109, 786–792.

Zhou, J., Smedley, G.T., 2006. Trabecular bypass: effect of Schlemm canal and collector channel dilation. J. Glaucoma 15, 446–455.